Effects of annealing and chemical doping on magnetic properties in Co-doped ZnO films

Y. Fukuma*
Yamaguchi Prefectural Industrial Technology Institute, 4-1 Asutopia, Ube 755-0195, Japan

F. Odawara, H. Asada, and T. Koyanagi
Department of Symbiotic Environmental Systems Engineering, Graduate School of Science and Engineering, Yamaguchi University, 2-16-1 Tokiwadai, Ube 755-8611, Japan

(Received 28 November 2007; revised manuscript received 2 July 2008; published 19 September 2008)

We have investigated the magnetic properties of Co-doped ZnO films on glass substrates prepared by sputtering. Annealing and chemical doping are performed to study the correlation between magnetism, conductivity, and defects. While as-deposited Co-doped ZnO film shows a paramagnetic behavior, the room-temperature ferromagnetism is induced by annealing in a H_2 atmosphere and is suppressed by annealing in air, indicating oxygen vacancy has strong relevance to the observed ferromagnetism. The ferromagnetism is also changed by impurity doping. The $s(p)$-d exchange interaction has been investigated by magnetotransport and magnetic circular dichroism (MCD) measurements. Large positive magnetoresistance at low temperatures and linear responses of both Hall effect and MCD to magnetic field suggest that the s-d exchange interaction gives rise to paramagnetic influence on electronic properties. Aggregation of a Co rich ZnO phase and a nanoscaled Co metal may give rise to the ferromagnetic behavior.

DOI: 10.1103/PhysRevB.78.104417 PACS number(s): 75.50.Pp, 72.15.Gd, 81.15.Cd, 85.75.−d

I. INTRODUCTION

Ferromagnetic semiconductors such as $Ga_{1-x}Mn_xAs$ and $In_{1-x}Mn_xAs$ have opened up the possibility of studying spintronics devices that utilize the polarized states of the electron-spin wave function in a semiconductor.[1–5] Ferromagnetism mediated by itinerant or weakly localized holes is well established by a mean-field model taking into account a p-d exchange hybridization and a spin-orbital interaction.[6] The Curie temperature (T_C) in the III–V alloys ranges up to 170 K.[7] According to the theoretical prediction based on the mean-field model, the room-temperature ferromagnetism would be realized for p-type GaN or ZnO with 5% Mn doping.[6]

ZnO is attracting much attention for its various applications to ultraviolet light emitters, high-power electronics, surface acoustic wave devices, gas sensing, and transparent electrodes for displays and solar cells.[8] The predicted ferromagnetism in the ZnO based magnetic semiconductors would allow us to add a new function of spin degrees of freedom in these devices. However, the experimental results are controversial. Ferromagnetic or paramagnetic behavior has been reported in various transition-metal (TM) doped ZnO films prepared by sputtering,[9–12] metal-organic chemical vapor deposition,[13,14] a sol-gel method,[15,16] pulsed-laser deposition,[17–25] and molecular-beam epitaxy.[26] A reasonable explanation of the conflicting data could be that the ferromagnetism appears sensitive to native defects such as interstitial zinc and oxygen vacancies in the host ZnO.[27] It is well known that the control of the stoichiometry in oxides is very difficult, causing many defects in the films. Actually, the ferromagnetism of the TM-doped ZnO films is suppressed by depositing or annealing in excess oxygen atmosphere, which eliminates the formation of oxygen deficiencies.[23–25]

One of the characteristic features of magnetic semiconductors is the $s(p)$-d exchange interaction between the sp band of the host semiconductor and the localized d electrons associated with magnetic ions. This exchange interaction yields spectacular magneto-optical and magnetotransport effects.[28] Magnetotransport and magnetic circular dichroism (MCD) measurements are extensively used for studying the $s(p)$-d exchange interaction of ferromagnetic semiconductors. However, for Co-doped ZnO films, relatively few studies have been reported on the magnetotransport and magneto-optical properties,[14,29,30] and the behavior is much different from that of conventional ferromagnetic semiconductors such as II–VI, III–V, and IV–VI alloys. Further investigation is necessary to elucidate the underlying mechanism of high T_C in the ZnO system. In this study, the magnetic properties of Co-doped ZnO films on glass substrates prepared by sputtering are reported. While as-deposited films show paramagnetic behavior, room-temperature ferromagnetism is induced by annealing in a H_2 atmosphere. Co-doped ZnO films with various carrier concentrations were also prepared by using dopants such as Al and Ga. To investigate the correlation between the ferromagnetism and the magnetotransport and magneto-optical properties, magnetoresistance and MCD measurements are performed on the ferromagnetic Co-doped ZnO films.

II. EXPERIMENT

Co-doped ZnO films were deposited on glass substrates (Corning 7059) by rf sputtering. The targets were a host ZnO disk (70 mm ϕ, 99.999%) on which Co chips (5×5 mm^2, 99.9%) were placed. In order to control the carrier concentration, pure ZnO, ZnO:Al (2 mol %), ZnO:Al (3 mol %), ZnO:Ga (1 mol %), and ZnO:Ga (2 mol %) targets were prepared by a spark plasma sintering technique. Fine powders of high purity ZnO (99.999%), Al_2O_3 (99.999%), and Ga_2O_3 (99.9999%) were mixed and were sintered at 700 °C under 30 MPa for 30 min in a Ar atmosphere. The relative density of the sintered disks determined by the Archimedes

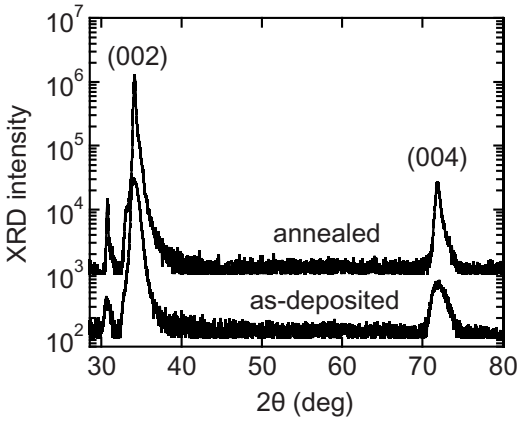

FIG. 1. X-ray diffraction patterns of as-deposited and H_2-annealed Co-doped ZnO films (Co 11%).

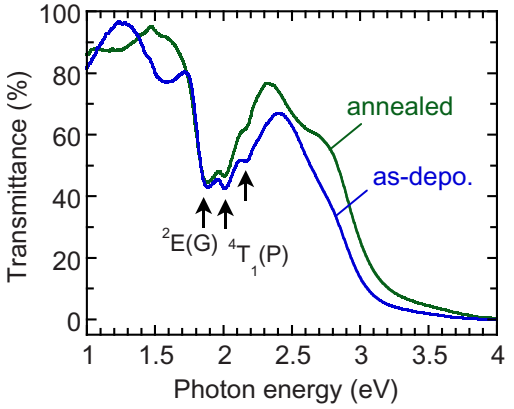

FIG. 2. (Color online). Optical transmittance spectra of as-deposited and H_2-annealed Co-doped ZnO films (Co 11%).

method was over 99%. The Co composition was controlled by changing the number of Co chips on the ZnO disk. The films were deposited at 300 °C and the deposition time was for 120 min. The rf power and the Ar gas pressure were fixed at 80 W and 10 mTorr, respectively. The typical deposition rate under these conditions was about 0.5 Å/s.

Crystallographic analysis was made by x-ray diffraction using a Cu $K\alpha$ source (RIGAKU RAD-B). The thickness was determined by using a field-emission scanning electron microscopy (HITACHI S-4700). The chemical composition was measured by electron probe microanalysis (HORIBA EMAX-7000). Optical transmittance spectra were measured on an ultraviolet-visible spectrometer at room temperature (SHIMAZU UV-3100PC). X-ray photoelectron spectroscopy was recorded at room temperature with a PHI Quantum 2000 spectrometer equipped with an Al $K\alpha$ source. A clean surface was obtained by Ar-ion sputtering in an ultrahigh vacuum before the measurement. The electrical measurements were performed on photolithographically patterned Hall-bar samples with 1 mm length and 200 μm width. The magnetization measurements were conducted on a superconducting quantum interference device magnetometer (Quantum Design MPMS7) at temperatures ranging from 4.2 to 300 K. The MCD measurements were carried out Faraday configuration with the magnetic field applied perpendicular to the film plane. The MCD spectra were taken at 1 T by switching the helicity of the incident light.

III. RESULTS AND DISCUSSION

Figure 1 shows a typical x-ray diffraction (XRD) pattern of the θ-2θ scan of the Co-doped ZnO films. The films are found to be c-axis oriented with the wurtzite structure, exhibiting the only (002) and (004) diffraction lines. There is no information about the formation of second phases. In order to control defects in the film, which would be associated with the magnetism, annealing was done at 350 °C for 30 min in a furnace. Annealing in a H_2 atmosphere improves the crystallinity of the Co-doped ZnO film, as shown in Fig. 1, while there was no distinct change of the crystallinity for the annealing in N_2 or O_2 atmosphere. The values of the full width at half maximum for the as-deposited and H_2-annealed films are 0.90° and 0.27°, respectively. It should be mentioned that a number of Co-doped ZnO films with different Co compositions were prepared and showed similar properties. Here, the Co (11%)-doped ZnO film which is the maximum Co composition in this study is used in discussing the annealing effect. The film was prepared by using the ZnO:Ga (1 mol %) target.

Figure 2 shows the optical transmittance spectra of the as-deposited and H_2-annealed Co-doped ZnO films. The transmittance in the visible region is also improved by the annealing. There was no change of the chemical composition within the resolution of our system (~1%). Therefore, the improvement of the crystallinity and transparency by the H_2 annealing can be attributed to a passivation of native defects in the Co-doped ZnO films. Absorption edges around 2.0 eV are attributed to d-d transition of $Co^{2+}(d^7)$ in tetrahedral coordination, as assigned to excitation from the $^4A_2$ (F) to the ^2E (G) and $^4T_1$ (P),[31] suggesting that most of Co ions are substituted for Zn sites in the host ZnO lattice. A vague transition of the band-edge region near 3.4 eV could be due to the metal (Co^{2+})-to-legand charge-transfer transition.[32]

To check the chemical state of Co ions in the Co-doped ZnO films, x-ray photoelectron spectroscopy (XPS) was done. Figure 3 shows the Co $2p$ core-level photoemission spectra of the as-deposited and H_2-annealed Co-doped ZnO films. The measurements were performed on the Co-doped ZnO films before and after Ar-ion sputtering, and thus are sensitive to the Co state near the surface and in the film. All the spectra exhibit nearly identical behavior: a spin-orbital doublet ($2p_{3/2}$, $2p_{1/2}$), each component of which shows a charge-transfer satellite on the higher binding energy side of the main peak. The presence of the satellite structure allows us to determine the valence state of Co ions because CoO and Co_3O_4 have different coupling into the two possible final states. The spectrum of Co_3O_4 exhibits a considerably lower intensity of the satellite peaks because of the more favorable lower binding energy of the $2p^53d^{n+1}L$ final state.[33] The Co $2p$ core-level spectra of the Co-doped ZnO films were similar to that of CoO,[34] implying that Co ions are substituted for Zn sites in the host ZnO lattice, which is consistent with the optical transmittance results. Zn $2p$ and O $1s$ spec-

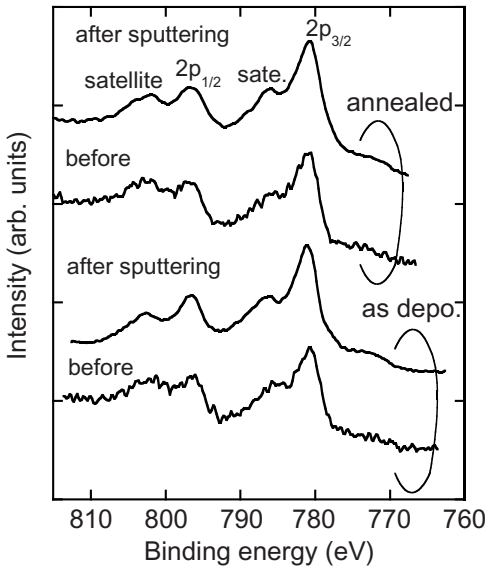

FIG. 3. X-ray photoemission spectra of Co 2*p* core level of Co-doped ZnO films (Co 11%).

tra were also taken and there was no change of the spectra between the as-deposited and H_2-annealed films. Therefore, the local chemical state of atoms in the H_2-annealed film may be identical to that of the as-deposited film.

The magnetization measurement results are shown in Fig. 4. All the measurements were performed on the same Co (11%)-doped ZnO film to avoid any errors from variations of the sample volume and the substrate background. First, the magnetization of the as-deposited film was measured (open triangles). After the as-deposited measurement, the film was annealed in the H_2 atmosphere and then measured (closed circles). Finally, the film was annealed in air at 400 °C for 10 min and then measured (open squares). The magnetization curves in Fig, 4(a) were taken at 4.2 K with the magnetic field applied parallel to the film plane. While the as-deposited film is found to be paramagnetic, the H_2-annealed film shows clear hysteresis behavior with a spontaneous magnetization of 4.2 emu/cm^3 and a coercive field of 800 Oe. The ferromagnetism is suppressed by annealing in air. Figure 4(b) shows the temperature dependence of the remanent magnetization, indicating that the Curie temperature of the H_2-annealed film is above room temperature. While the hysteresis loop shows a low squareness ratio (remanent/saturation) with a small moment and the temperature dependence of the magnetization shows a concave curve, there were no traces of a microscopic precipitation of any binary magnetic alloys such as antiferromagnetic CoO,[35] ferrimagnetic Co_3O_4,[36] or ferromagnetic ZnCo,[37] as deduced from the x-ray diffraction, optical, and XPS measurements.

In order to understand the influence of the H_2 annealing on the defects, photoluminescence (PL) measurements were done using a XeCl excimer laser (308 nm) at 4.2 K. Figure 5 shows PL spectra of as-deposited and H_2 annealed ZnO films. In this measurement, the host ZnO film prepared under the same growth conditions as the Co-doped ZnO films is used to get a clear PL spectrum. For the as-deposited film, deep-level related emission peaks at around 2.4 eV and a

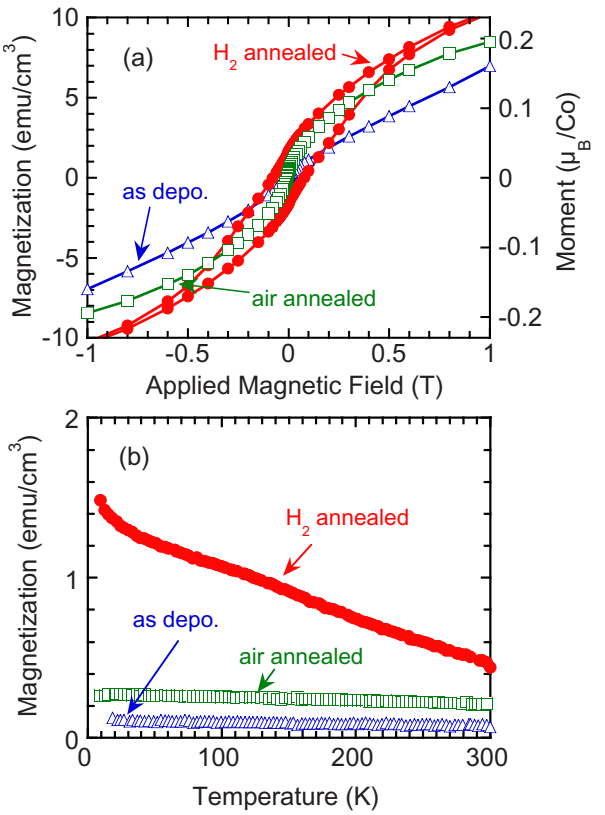

FIG. 4. (Color online) (a) Magnetization curves at 4.2 K and (b) temperature dependence of remnant magnetization for Co-doped ZnO films (Co 11%). All the measurements were performed on the same sample.

broad peak at 3.0 eV are observed. The deep-level emission is related to oxygen vacancies and zinc interstitials,[38] and is not suppressed by the H_2 annealing. On the other hand, the peak at 3.0 eV is related to defects associated with an oxygen-rich composition such as a Zn vacancy,[39] and is drastically changed by the H_2 annealing. The two distinct peaks at around 3.34 and 3.37 eV for the H_2 annealed film can be identified as a bound exciton emission due to the recombination of excitons trapped in shallow donor levels and the free

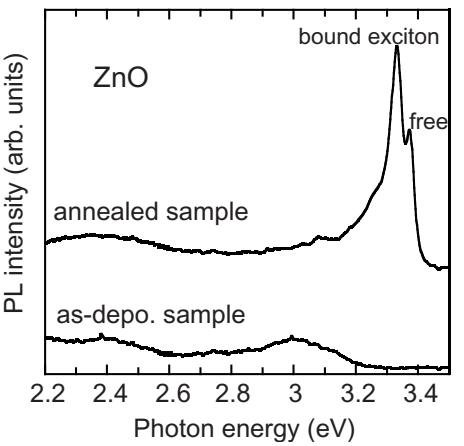

FIG. 5. Photoluminescence of as-deposited and H_2-annealed ZnO films at 4.2 K.

TABLE I. Electronic properties for Co-doped ZnO films with dopant. The resistivity ρ, electron concentration n, and mobility μ are determined by the Hall measurements at room temperature.

Sample	Co (%)	Dopant (%)	$\rho(\Omega\ \mathrm{cm})$	$n(\mathrm{cm}^{-3})$	$\mu(\mathrm{V\ s/cm}^2)$
Z184	6.6	0	3.72×10^{-2}	1.51×10^{19}	11.0
Z187	5.7	3.1 (Al)	3.10×10^{-3}	1.80×10^{20}	11.2
Z191	7.0	1.1 (Al)	4.55×10^{-3}	7.46×10^{19}	18.4
Z199	5.0	1.5 (Ga)	6.05×10^{-3}	7.33×10^{19}	14.1

exciton, respectively,[40] implying a high crystalline quality despite the polycrystalline films. Therefore, the H_2 annealing passivates the oxygen-rich related defects in the as-deposited film and activates the shallow donor impurities, causing high n-type conductivity. This result is consistent with the XRD and transmittance results, i.e., the crystalline quality is improved by the H_2 annealing. Therefore, for the as-deposited Co-doped ZnO film, the defects related to the oxygen-rich composition could suppress the ferromagnetic ordering. The H_2 annealing compensates the oxygen-related defects and then activates the shallow donor impurities such as oxygen vacancies and n-type dopants, causing the ferromagnetism. The resistivity (over 10^2 Ω cm) of the as-deposited film was drastically decreased to 3.88×10^{-3} Ω cm by H_2 annealing. It should be mentioned that a higher temperature of over 350 °C and a longer annealing time in a H_2 atmosphere caused a significant degradation of the optical and crystalline properties of the Co-doped ZnO films.

The ferromagnetism of Mn-doped magnetic semiconductors with p-type conduction is associated with the carrier concentration via the Ruderman-Kittel-Kasuya-Yosida (RKKY) interaction.[41–43] In the ZnO system, since the oxygen deficiency causes high n-type conduction it is hard to determine the origin of the ferromagnetism, i.e., the defects or the carrier concentration. To study the carrier-concentration dependence of the ferromagnetic properties, Co (~6%)-doped ZnO films with various carrier concentrations were prepared, as summarized in Table I. All the samples were annealed at a H_2 atmosphere and then showed high n-type conductivity. The carrier concentration increased with the dopant concentration. Figure 6 shows the magnetization curves at room temperature. The magnetic field was applied parallel to the film plane. The saturation magnetization increases slightly with increasing carrier concentration while the coercive field is fixed around 100 Oe.

One of the characteristic features of magnetic semiconductors is the $s(p)$-d exchange interaction, which yields a large negative magnetoresistance (MR) due to the formation of a magnetic polaron,[44,45] a clear anomalous Hall effect which is coincident with the magnetism,[46,47] and a large magneto-optical effect due to the large Zeeman splitting.[48–50] Figure 7 shows MR measurement results of the Co-doped ZnO films with various carrier concentrations at 2.7 K when the magnetic field was applied perpendicular to the film plane. For Z184, the MR shows a complicated behavior containing positive and negative components, as reported for paramagnetic Mn- or Co-doped ZnO films.[51–53] For the other Co-doped ZnO films with dopants, the positive MR decreases with increasing carrier concentration. According to the first principle calculation of MR taking into account the s-d exchange interaction in TM-doped ZnO, the presence of a giant spin splitting of the conduction band gives rise to large positive MR.[53] In the case of conventional ferromagnets, MR exhibits a negative component with a hysteretic behavior due to the suppression of a spin-disorder scattering or anisotropic MR dependent on the relative orientation of the current and the magnetization by the spin-orbit interaction.[54] Therefore, the positive MR without hysteresis in the ferromagnetic Co-doped ZnO films suggests that MR is mainly dominated by the s-d exchange interaction between paramagnetic Co moments and itinerant or weakly localized electrons. Figure 8 shows one of the examples of MR as a function of temperature for Co (5%)-doped ZnO with $n=3.28\times10^{19}$ cm^{-3}. The MR displays a change from positive

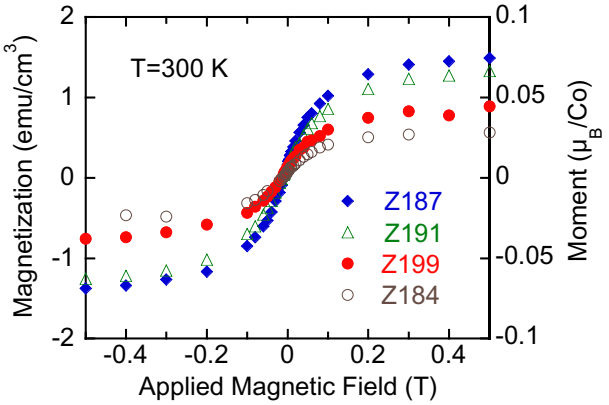

FIG. 6. (Color online) Magnetization curves of Co-doped ZnO films (Co~6%) with different carrier concentrations, at 300 K.

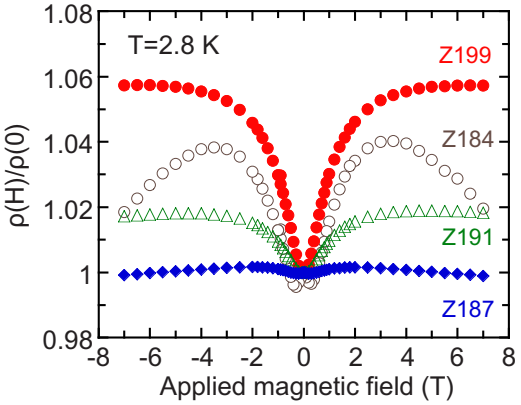

FIG. 7. (Color online) Magnetoresistance of Co-doped ZnO films (Co~6%) with different carrier concentrations, at 2.7 K.

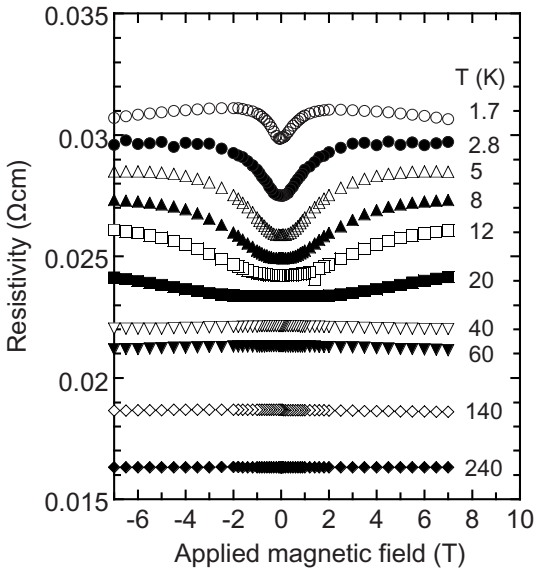

FIG. 8. Magnetoresistance of Co-doped ZnO films (Co 5%) with $n=3.28\times10^{19}$ cm^{-3} as a function of temperature.

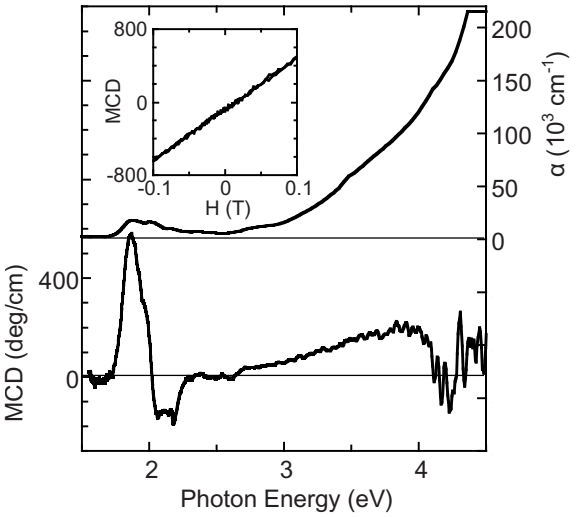

FIG. 9. Magnetic circular dichroism spectra at 1 T and optical-absorption spectra at room temperature for the Co-doped ZnO film (Co 9.3%). The inset shows the magnetic field dependence of the magnetic circular dichroism at 1.87 eV.

to negative as the temperature increases. On the other hand, the magnetization does not show a drastic temperature dependence, as shown in Fig. 4(b). There is no relationship between the ferromagnetism and the MR. Moreover, the temperature dependence of the MR is quite similar to that predicted for paramagnetic TM-doped ZnO.[53] The Hall effect was also measured on various Co-doped ZnO films at different temperatures ranging from 2 to 300 K. All the results showed a linear behavior, i.e., there is no distinct anomalous Hall effect in the ferromagnetic Co-doped ZnO films.

Figure 9 shows MCD and absorption spectra of the ferromagnetic Co-doped ZnO film at room temperature. The MCD spectrum consists of Co^{2+} d-d transitions around 2.0 eV and a near-band-edge transition around 3.5 eV. The weak positive peak near the band-edge transition at room temperature is also reported for paramagnetic $Zn_{1-x}Co_xO$.[55] The MCD intensity changes linearly with magnetic field, as shown in the inset of Fig. 9, implying that the ferromagnetism does not have a magneto-optical response. There was no hysteresis behavior in MCD for all the ferromagnetic Co-doped ZnO films studied here.

The paramagnetic response of the MR, the Hall effect, and the MCD imply that the ferromagnetism of the Co-doped ZnO films does not give rise to the $s(p)$-d exchange interaction, which is reported for conventional ferromagnetic semiconductors.[44–50] Therefore, the mechanism of ferromagnetic ordering for the Co-doped ZnO films is different from that of the others, where the magnetization increases with increasing carrier concentration. The fact that there is no correlation between the ferromagnetism and the magneto-optical and magnetotransport properties, and the fact that high-quality Co-doped ZnO epitaxial layers with high n-type conduction exhibited a paramagnetic behavior[56] suggest that the free carrier does not give rise to the ferromagnetism in this system. An interesting physical model for explaining the mechanism of the ferromagnetism in oxides is the spin-split donor impurity band model proposed by Coey *et al.*[27] At a percolation threshold which is associated with the defect and magnetic ion concentrations, a long-range ferromagnetic order is induced by overlapping the polarons due to high dielectric constant in oxides, creating a spin-split impurity band. However, even with high Co composition over few percentage and high defect concentration in the polycrystalline Co-doped ZnO films in this study, the ferromagnetic ordering is of short-range type because of the nonsquare magnetization curve with a small moment and the concave M-T curve.

On the basis of a conventional mean-field model of the ferromagnetism, the exchange length of the ferromagnetic order is proportional to the exchange integral J_{sd}, which is related to T_C.[57] The J_{sd} of Co-doped ZnO could be strong due to high T_C and should cause a long-range order. However, the observed ferromagnetic behavior seems to be short-range order, even though the magnetic concentration (Co $\sim 10\%$) is high enough to induce the long-range order. Sato *et al.* proposed that the range of exchange interaction in the wide-gap system, forming the impurity band in the gap, is very short order because of the exponential decay of the wave function.[58] Such a localization of carriers will form a magnetic polaron by the strong sp-d exchange interaction. However, negative MR by magnetic polarons is absent in the magnetotransport measurements even at low temperature with a high magnetic field. Therefore, an interpretation based on an inhomogeneous ferromagnetism is preferred to understand the ferromagnetism.[59] While there is no information on the formation of macroscopic second phases from the XRD and XPS measurements, the oxygen-related defects induced by the H_2 annealing can be attributed to the aggregation of a Co rich ZnO phase and a nanoscaled Co metal.

IV. CONCLUSIONS

The magnetic properties of Co-doped ZnO films on glass substrates prepared by sputtering are investigated. The Co-

doped ZnO films are found to be *c*-axis oriented with the wurtzite structure. While as-deposited films show a paramagnetic behavior, the room-temperature ferromagnetism is induced by annealing in a H_2 atmosphere, and is suppressed by annealing in air. The H_2 annealing passivates oxygen-rich related defects and activates donor impurities associated with oxygen deficiencies and dopants, causing high *n*-type conduction. We have prepared ferromagnetic Co-doped ZnO films with various carrier concentrations by using dopants such as Ga and Al. The saturation magnetization increases slightly with increasing carrier concentration. However, there is no correlation between the ferromagnetism and the magnetotransport and magneto-optical properties; large positive magnetoresistance at low temperatures, linear behaviors of the Hall resistivity, and the MCD with the applied magnetic field are observed. The ferromagnetic order is of short-range type because of the nonsquare magnetization curves with a small Co moment and the concave magnetization vs temperature curve. While there is no trace of the formation of a microscopic second phase from the XRD, optical transmittance, and XPS measurements, the aggregation of a Co rich ZnO phase and a nanoscaled Co metal may give rise to the ferromagnetic behavior.

ACKNOWLEDGMENTS

We thank Y. Yamada and T. Taguchi for the help with PL measurements, K. Nagao for the help with XPS measurements, T. Matsushita, S. Otabe, and M. Kiuchi for the help with SQUID measurements, and K. Ando and H. Saito for the help with MCD measurements.

*Present address: Advanced Science Institute, RIKEN, 2-1 Hirosawa, Wako 351-0198; yfukuma@riken.jp

[1] H. Munekata, H. Ohno, S. von Molnár, A. Segmuller, L. L. Chang, and L. Esaki, Phys. Rev. Lett. **63**, 1849 (1989).
[2] H. Ohno, A. Shen, F. Matsukura, A. Oiwa, A. Endo, S. Katsumoto, and Y. Iye, Appl. Phys. Lett. **69**, 363 (1996).
[3] H. Ohno, Science **281**, 951 (1998).
[4] Y. Ohno, D. K. Young, B. Beschoten, F. Matsukura, H. Ohno, and D. D. Awschalom, Nature (London) **402**, 790 (1999).
[5] H. Ohno, D. Chiba, F. Matsukura, T. Omiya, E. Abe, T. Dietl, Y. Ohno, and K. Ohtani, Nature (London) **408**, 944 (2000).
[6] T. Dietl, H. Ohno, F. Matsukura, J. Cibert, and D. Ferrand, Science **287**, 1019 (2000); T. Dietl, H. Ohno, and F. Matsukura, Phys. Rev. B **63**, 195205 (2001).
[7] K. Y. Wang, R. P. Campion, K. W. Edmonds, M. Sawicki, T. Dietl, C. T. Foxon, and B. L. Gallagher, in *Physics of Semiconductors: 27th International Conference on the Physics of Semiconductors*, edited by J. Menéndez and C. G. Van de Walle, AIP Conf. Proc. No. 772 (AIP, New York, 2005), p. 333.
[8] See, for example, S. J. Pearton, C. R. Abernathy, M. E. Overberg, G. T. Thaler, D. P. Norton, N. Theodeoropoulou, A. F. Hebard, Y. D. Park, F. Ren, J. Kim, and L. A. Boatner, J. Appl. Phys. **93**, 1 (2003); S. J. Pearton, C. R. Abernathy, D. P. Norton, N. Theodeoropoulou, A. F. Hebard, Y. D. Park, L. A. Boatner, and J. D. Budai, Mater. Sci. Eng., R. **40**, 137 (2003).
[9] Y. M. Cho, W. K. Choo, H. Kim, D. Kim, and Y. E. Ihm, Appl. Phys. Lett. **80**, 3358 (2002).
[10] X. M. Cheng and C. L. Chien, J. Appl. Phys. **93**, 7876 (2003).
[11] C. Liu, F. Yun, B. Xiao, S. J. Cho, Y. T. Moon, H. Morkoc, M. Abouzaid, R. Ruterana, K. M. Yu, and W. Walukiewicz, J. Appl. Phys. **97**, 126107 (2005).
[12] Z. B. Gu, C. S. Yuan, M. H. Lu, J. Wang, S. T. Zhang, S. H. Zhu, Y. Y. Zhu, and Y. F. Chen, J. Appl. Phys. **98**, 053908 (2005).
[13] A. B. Pakhomov, B. K. Roberts, A. Tuan, V. Schutthanandan, D. Mcready, and S. Thevuthasan, S. A. Chambers, and K. M. Krishnana, J. Appl. Phys. **95**, 7393 (2004).
[14] A. C. Tuan, J. D. Bryan, A. B. Pakhomov, V. Shutthanandan, S. Thevuthasan, D. E. McCready, D. Gaspar, M. H. Engelhard, J. W. Rogers, K. Krishnan, D. R. Gamelin, and S. A. Chambers, Phys. Rev. B **70**, 054424 (2004).
[15] H. J. Lee, S. Y. Jeong, C. R. Cho, and C. H. Park, Appl. Phys. Lett. **81**, 4020 (2002).
[16] J. H. Park, M. G. Kim, H. M. Jang, S. Ryu, and Y. M. Kim, Appl. Phys. Lett. **84**, 1338 (2004).
[17] K. Ueda, H. Tabata, and T. Kawai, Appl. Phys. Lett. **79**, 988 (2001).
[18] Z. Jin, T. Fukumura, M. Kawasaki, K. Ando, H. Saito, T. Sekiguchi, Y. Z. Yoo, M. Murakami, Y. Matsumoto, and H. Koinuma, Appl. Phys. Lett. **78**, 3824 (2001).
[19] H. Saeki, H. Tabata, and T. Kawai, Solid State Commun. **120**, 439 (2001).
[20] S. W. Jung, S. J. An, G. C. Yi, C. U. Jung, S. I. Lee, and S. Cho, Appl. Phys. Lett. **80**, 4561 (2002).
[21] J. H. Kim, H. Kim, D. Kim, Y. E. Ihm, and W. K. Choo, J. Appl. Phys. **92**, 6066 (2002).
[22] A. Tiwari, C. Jin, A. Kvit, D. Kumar, J. F. Muth, and J. Narayan, Solid State Commun. **121**, 371 (2002).
[23] M. Venkatesan, C. B. Fitzgerald, J. G. Lunney, and J. M. D. Coey, Phys. Rev. Lett. **93**, 177206 (2004).
[24] N. H. Hong, J. Sakai, N. T. Huong, N. Poirot, and A. Ruyter, Phys. Rev. B **72**, 045336 (2005).
[25] S. Ramachandran, J. Narayan, and J. T. Prater, Appl. Phys. Lett. **88**, 242503 (2006).
[26] A. C. Mofor, A. El-Shaer, A. Bakin, A. Waag, H. Ahlers, U. Siegner, S. Sievers, M. Albrecht, W. Schoch, N. Izyumskaya, V. Avrutin, S. Sorokin, S. Ivanov, and J. Stoimenos, Appl. Phys. Lett. **87**, 062501 (2005).
[27] J. M. D. Coey, M. Venkatesan, and C. B. Fitzgerald, Nat. Mater. **4**, 173 (2005).
[28] See, for example, J. K. Furdyna, J. Appl. Phys. **64**, R29 (1988); W. J. M. de Jonge and H. J. M. Swagten, J. Magn. Magn. Mater. **100**, 322 (1991).
[29] K. Ando, H. Saito, V. Zayets, and M. C. Debnath, J. Phys.: Condens. Matter **16**, S5541 (2004).
[30] K. R. Kittilstved, W. K. Liu, and D. R. Gamelin, Nat. Mater. **5**, 291 (2006).
[31] P. Koidl, Phys. Rev. B **15**, 2493 (1977).
[32] D. A. Schwartz, N. S. Norberg, Q. P. Nguyen, J. M. Parker, and

D. R. Gamelin, J. Am. Chem. Soc. **125**, 13205 (2003).
[33] M. Oku and Y. Sato, Appl. Surf. Sci. **55**, 37 (1992).
[34] M. A. Langell, M. D. Anderson, G. A. Carson, L. Peng, and S. Smith, Phys. Rev. B **59**, 4791 (1999).
[35] H. Bizette, Ann. Phys. (Paris) **1**, 295 (1946).
[36] W. Kundig, M. Kobelt, H. Appel, G. Constabaris, and R. H. Lindquist, J. Phys. Chem. Solids **30**, 819 (1969).
[37] J. Schramm, Z. Metallkd. **33**, 46 (1941).
[38] H. J. Egelhaaf and D. Oelkrug, J. Cryst. Growth **161**, 190 (1996).
[39] S. H. Jeong, B. S. Kim, and B. T. Lee, Appl. Phys. Lett. **82**, 2625 (2003).
[40] D. W. Hamby, D. A. Lucca, M. J. Klopfstein, and G. Cantwell, J. Appl. Phys. **93**, 3214 (2003).
[41] M. Ruderman and C. Kittel, Phys. Rev. **96**, 99 (1954).
[42] T. Kasuya, Prog. Theor. Phys. **16**, 45 (1956).
[43] K. Yosida, Phys. Rev. **106**, 893 (1957).
[44] S. von Molnar, J. Supercond. **14**, 199 (2001).
[45] A. Oiwa, S. Katsumoto, A. Endo, M. Hirasawa, Y. Iye, H. Ohno, F. Matsukura, A. Shen, and Y. Sugawara, Solid State Commun. **103**, 209 (1997).
[46] A. Oiwa, A. Endo, S. Katsumoto, Y. Iye, H. Ohno, and H. Munekata, Phys. Rev. B **59**, 5826 (1999).
[47] Y. Fukuma, M. Arifuku, H. Asada, and T. Koyanagi, J. Appl. Phys. **91**, 7502 (2002).
[48] P. Fumagalli and H. Munekata, Phys. Rev. B **53**, 15045 (1996).
[49] K. Ando, T. Hayashi, M. Tanaka, and A. Twardowski, J. Appl. Phys. **83**, 6548 (1998).
[50] H. Saito, V. Zayets, S. Yamagata, and K. Ando, Phys. Rev. Lett. **90**, 207202 (2003).
[51] Z. Jin, T. Fukumura, K. Hasegawa, Y. Z. Yoo, K. Ando, T. Sekiguchi, P. Ahmet, T. Chikyow, T. Hasegawa, H. Koinuma, and M. Kawasaki, J. Cryst. Growth **237-239**, 548 (2002).
[52] J. H. Kim, H. Kim, D. Kim, Y. E. Ihm, and W. K. Choo, Physica B (Amsterdam) **327**, 304 (2003).
[53] T. Andrearczyk, J. Jaroszynski, G. Grabecki, T. Dietl, T. Fukumura, and M. Kawasaki, Phys. Rev. B **72**, 121309(R) (2005).
[54] T. R. Mcguire and R. I. Potter, IEEE Trans. Magn. **11**, 1018 (1975).
[55] K. Ando, H. Saito, Z. Jin, T. Fukumura, M. Kawasaki, Y. Matsumoto, and H. Koinuma, Appl. Phys. Lett. **78**, 2700 (2001).
[56] Z. W. Jin, T. Fukumura, K. Hasegawa, Y. Z. Yoo, K. Ando, T. Sekiguchi, P. Ahmet, T. Chikyow, T. Hasegawa, H. Koinuma, and M. Kawasaki, J. Cryst. Growth **237-239**, 548 (2002).
[57] B. D. Culity, *Introduction of Magnetic Materials* (Addison-Wesley, Reading, MA, 1972), Chap. 11, pp. 383–438.
[58] K. Sato, W. Schweika, P. H. Dederichs, and H. Katayama-Yoshida, Phys. Rev. B **70**, 201202(R) (2004).
[59] T. Dietl, Nat. Mater. **5**, 673 (2006).